FORMULATION AND EVALUATION OF NANOSTRUCTURED LIPID CARRIERS LOADED WITH REPAGLINIDE

Mohamed A. Nasr-Eldin[1, 2, 3 *], Ibrahim A. Elbahwy[1], Ahmed M. Samy [1], Mohsen M. I. Afouna[1].

[1] Department of Pharmaceutics and Pharmaceutical Technology, College of Pharmacy (Boys), Al-Azhar University, 1 El-Mokhayam El-Daem St., Nasr City, P.O. Box 11884, Cairo, Egypt.

[2] Military Medical Academy

[3]Armed Forces Pharmaceutical Factory

***Corresponding author**: E.mail: mohamednasreldin.224@azhar.edu.eg

ABSTRACT

Repaglinide (REP) is a potent medication for treating diabetes (BCS class II) that has a low oral bioavailability of less than 55% due to its poor solubility and significant metabolism in the liver during its first pass. The objective of this study was to develop a nanocarrier system called nanostructured lipid carriers loaded with repaglinide (REP-NLCs) that provides the benefits of prolonged drug release and enhanced oral bioavailability. Conducting solubility experiments allowed for the identification of suitable lipids and surfactants for the formulation of NLCs. The REP-NLCs were synthesized using hot homogenization followed by ultrasonication procedures and subsequently analyzed for their size, zeta potential, polydispersity index (PDI), and drug entrapment efficiency (E.E). The results demonstrated that altering the lipid or surfactant type had a significant impact on the entrapment efficiencies, particle size, and release behavior of the NLCs. The average particle size varied between 59.1 ± 3.2 and 898.4 ± 40.3 nm. The particles exhibited a negative charge, with zeta potential values ranging from −32.27 ± 1.01 to −26.13 ± 7.37 mV. The in vitro release of all REP-NLC formulas exhibited a biphasic time-dependent pattern. The E.E varied between 70.11 ± 5.3 and 85.32 ± 4.6 %. REP-NLCs exhibited prolonged drug release compared to the dissolution of REP suspension.

Keywords: Repaglinide (REP), Nanostructured lipid carriers (NLCs), emulsification–ultrasonification, Oral route.

Introduction

The oral route administration provides a treasured option for treating numerous diseases as it shows compliance, cost effectiveness and ease of administration and is considered as the most acknowledged route for drug administration. Drug candidates that are stable in a gastric environment and possess adequate hydrophilic lipophilic balance to cross the intestinal epithelium membrane in the absence of significant GI tract (GIT) irritation and toxicity signs are ideal candidates for oral delivery. Miserably, more than 40% of API emerged from the drug discovery are not appropriate for the drug delivery via oral route as a consequence of their hydrophobic nature and present poor oral bioavailability ***(Kesharwani et al., 2022)***.

Diabetes mellitus is a widespread, persistent ailment with serious life-threatening results on different parts/functions all over the body. The maximum number of diabetic sufferers is observed to be type II diabetes mellitus, i.e., (non-insulin-dependent). To control this type of diabetes, various classes of oral anti-diabetic drugs are commonly utilized in the market to decrease dosage and adverse effects accompanying the drug. Belongs to this various medications available from different classes being utilized, such as Sulfonylurea Thiazolidinedione, Biguanide Meglitinide analogs, and Glucosidase inhibitors etc. ***(Ebrahimi et al., 2015).***

The REP is an oral medicament utilized to treat type 2 diabetes; shows poor water solubility is associated with class II Biopharmaceutical Classification System. It is absorbed rapidly in the gastrointestinal tract (GI) and has a high hepatic first pass effect with a mean bioavailability of about 50–60%. It is eliminated fast from the body by the biliary excretion route. Its mechanism of action is partially similar to sulphonylureas like glibenclamide which stimulates the release of insulin from the pancreatic beta cells by closing ATP-dependent potassium channels in the presence of glucose. The half-life of REP is about 1 h, so it should be used 3–4 times in a day ***(Pandey et al., 2020)***.

For bioavailability enhancement of REP, the researchers have attempted various approaches to overcome the challenges associated with oral delivery of Repaglinide, such as nanoemulsions, self-nano emulsifying systems, nanocrystals, solid lipid nanoparticles, and NLC **(Kesharwani *et al.,* 2022)**. The solid lipid nanoparticles (SLNs) and Nanostructured lipid carriers (NLCs), both types of lipids nanocarriers, exhibit the great potential to improve the therapeutic effectiveness of numerous drugs by various routes of administration like oral, parenteral and dermal. Their main benefits such as the chance of controlled and targeting drug release, potential incorporation of hydrophobic as well as hydrophilic drugs, amazing biocompatibility and low biotoxicity **(Akel et al., 2021)**.

NLCs are second-generation SLNs with an unstructured matrix, high drug loading, and long-term drug stability in comparison to SLNs and other colloidal systems. NLCs are innovative drug delivery systems composed of both solid and liquid lipids. NLCs offer several advantages over conventional drug carriers, including increased solubility, enhanced storage stability, improved permeability and bioavailability, reduced adverse effects, prolonged half-life, and targeted delivery to specific tissues ***(Viegas et al., 2023).***

Experimental

Materials

Repaglinide, Bees wax, Cetyl alcohol, Oleic acid, Peppermint oil, Miglyol 840, Lutrol®F68, Lutrol®F127, Carboxymethyl cellulose (CMC) and Tween 20 were kindly gifted by Egyptian International Pharmaceutical Industrial Company (EIPICO) (Egypt). Precirol®ATO 5, Maisine®CC, Comperitol®888 ATO, Labrafac™ PG, Labrafac™ Lipophile WL 1349, Capryol™90, Labrasol®ALF, Gelucire®50/13 and Labrafil®M2130CS were kindly gifted by Gattefosse (France). Solvents (distilled water, methanol) of HPLC analytical grade were purchased from Fisher Scientific Company (USA). Potassium phosphate monobasic was purchased from Alpha Chemika (India). Ethanol absolute (HPLC grade) was purchased from Merck (Germany). All other chemicals were used of analytical grade.

UV-scanning of REP

The UV spectrum of REP was carried out in methanol solution; in brief, repaglinide was weighed accurately at 10 mg and transferred into methanol solution in a 200-ml volumetric flask. The solution of 50 µg/ml was kept in a cuvette. The UV spectrum was recorded in the wave length range of 200–400 nm by UV visible spectrophotometer (Shimadzu, the model UV-1800 PC, Kyoto, Japan) against a blank methanol solution ***(Shaikh et al., 2020)***.

Construction of calibration curve of REP in methanol

Fifty mg of (REP) was dissolved in the least amount of methanol, and the volume was increased up to 1000 ml with methanol (stock solution). Samples of 0.5, 1, 1.5, 2, 2.5, 3, 3.5, 4, 4.5, and 5 ml were taken and completed to 10 ml with methanol to give solutions containing 2.5, 5, 7.5, 10, 12.5, 15, 17.5, 20, 22.5, and 25 µg/ml, respectively. The absorbance of REP concentrations was determined spectrophotometrically at the calculated λ_{max} of REP (242 nm) using methanol as a blank ***(Shaikh et al., 2020).*** A calibration curve was plotted. The experiment was repeated in triplicate.

Construction of calibration curve of RPG in PBS pH 6.8 + 0.5% Tween 20

Fifty mg of (REP) was dissolved in the least amount of phosphate buffered saline (PBS) pH 6.8+ 0.5% Tween 20, and the volume was increased to 1000 ml with PBS pH 6.8 + 0.5% Tween 20 (stock solution). Samples of 0.5, 1, 1.5, 2, 2.5, 3, 3.5, 4, 4.5, and 5 ml were taken and completed to 10 ml with methanol to give solutions containing 2.5, 5, 7.5, 10, 12.5, 15, 17.5, 20, 22.5, and 25 µg/ml, respectively. The absorbance of REP concentrations was determined spectrophotometrically at the calculated λ_{max} of REP (242 nm) using PBS pH 6.8 + 0.5% Tween 20 as a blank. A calibration curve was plotted. The experiment was repeated in triplicate.

Solubility analysis of Repaglinide in solids lipids

The solid lipid screening was carried out by quantifying the saturation solubility of REP in different solid lipids, which was determined by the test tube method. A precisely weighted amount of the REP (100 mg) was putted in the test tube, and then the solid lipid was added in increments of 250 mg to the test tube, which could be heated to 4-5 °C above the melting point of the solid lipid by saving it in a controlled-temperature water bath (Water path 4050, Romo, Cairo, Egypt), until it failed to dissolve further in it. The quantity of solid lipid required to solubilize the drug in its molten state was recorded. The full dissolution state was completed by the formation of a clear and transparent solution. The experiments were conducted in triplicate ***(Luo et al., 2022)***.

Solubility analysis of Repaglinide in liquid lipids

Screening of liquid lipids was achieved by determining the saturation solubility of REP in various oils, which was performed by adding an excess amount of drug in small glass vials containing a fixed volume (5 ml) of different liquid lipids. The vials were strictly closed and incubated in adjusted mechanical shaker (Oscillating thermostatically controlled shaker, Gallent Kamp, England) for 72 h at 37 °C with continuous agitation at 100 rpm. Then these vials were centrifuged at high-speed using (Biofuge Primo centrifuge maximum 17.000 rpm, England) centrifuged at 10,000 rpm for 15 min. followed by collection of supernatants by passing through a membrane filter of 0.45 μm diameter. Finally, the supernatant was aspirated and determined spectrophotometrically at the calculated λ_{max} of REP (242 nm). The experiments were conducted in triplicate ***(Dash et al., 2022)***.

Physical compatibility of solid lipids and liquid lipids

The miscibility of selected solid lipids and liquid lipids that possess the maximum affinity for the drug could be achieved. A constant ratio of 1:1 of solid lipids and liquid lipids were mixed and melted in different glass tubes. The molten binary lipid mixture was allowed to congeal at room temperature. After that, the glass tubes were visually determined for the absence of divided layers in the congealed lipid mass. Furthermore, the miscibility between solid lipid and liquid lipid was inspected by smearing a cooled sample of congealed lipid mixture onto a filter paper, followed by visual observation to clear the presence of any oil droplets on the filter paper ***(Mathur et al., 2020)***.

Selection of a binary lipid phase ratio

The ratio of selected solid lipids and liquid lipids was determined based on the melting point of the binary lipid mixture. Solid and liquid lipids were selected based on the melting point of the mix. Selected solid and liquid lipids were blended in a ratio varying from 90:10 to 10:90. By magnetic stirrer (Magnetic stirrer, Wise-stir, Model MSH-20D, Hot plate stirrer, Korea), lipid mixture was agitated at 1200 rpm for an hour at 80 °C. After 1hr, the lipid mixture was cooled and poured into filter paper. Then the solid mixture was inspected visually for the occurrence of any oil droplets on it. A

binary mixture with a melting point above 40°C and no evidence of oil droplets on the filter paper was chosen for NLC development ***(Dash et al., 2022).***

Screening of surfactant

The surfactant used for the fabrication of NLCs should be screened to be selected depending on its ability to emulsify a solid-liquid binary lipid mixture. A binary lipid mixture (100 mg) was dissolved in 3 ml of methylene chloride and added to 10 ml of 5% surfactant solutions, then stirred by applying a magnetic stirrer. The organic layer was evaporated at 40°C, and the remaining suspensions were diluted with 10-fold distilled water. The transmittance percent of the resultant samples was determined using a UV-Vis spectrophotometer (Shimadzu, the model UV-1800 PC, Kyoto, Japan) at 510 nm ***(Anwar et al., 2019)***.

Fabrication of Repaglinide nanostructured lipid carriers (REP-NLC)

REP nanostructured lipid carriers (REP-NLC) were prepared by hot homogenization followed by ultrasonication techniques ***(Dash et al., 2022)***, but with a few modifications. Briefly, the weighted amount of the selected solid-liquid binary lipid mixture (4% w/w) was melted at 5 °C above the melting point of the solid lipid. A known concentration of REP (5% w/w of lipids) (200mg) was dissolved in the prepared oil phase (a 4% w/w mixture of solid and liquid lipids). The aqueous phase containing selected surfactant (2.5% w/w) was heated to the same temperature and added (dropwise) to the oil phase under magnetic stirring at 1500 rpm for 10 min. After that, homogenization of the resultant pre-emulsion was performed at a high speed of about 20,000 rpm using an Ultra-Turrax T25 homogenizer (Wise Mix™ HG15A, Daihan Scientific, Seoul, Korea) for 15 min. The resultant o/w nanoemulsion was subjected to probe sonicator (ultrasonic processor, GE130, probe CV18, USA) at 60% amplitude for 10 min. The obtained NLC dispersion was cooled down to room temperature and stored at 4 °C **(Yu et al., 2023)**.

Physicochemical characterization of REP-NLCs

Particle size, polydispersity index and zeta potential analysis

The liquid NLC formulation's particle size (PS), PDI, and zeta potential (ZP) were measured using the Malvern Zetasizer (Nano ZS; Malvern Instruments, Malvern, UK) at room temperature. The particle size was determined using the photon correlation spectroscopic (PCS) technique ***(Dash et al., 2022)***, while the ZP was measured using the electrophoretic light scattering technique ***(Rahman et al., 2023)***.

Encapsulation efficiency (EE)

The E.E of NLCs represents the proportion of the drugs that has been trapped within the lipid matrix's core. The drug's entrapment percentage in NLC formulations was measured using high-speed cooling centrifugation (Beckman Instruments TLX-120 Optima Ultracentrifuge) centrifuged at 120000 rpm for 2 hours at 4 °C. The concentration of the unbound drug in the supernatant was determined using a double

beam UV-Visible Spectrophotometer. The proportion of the drug that was successfully entrapped was determined using the following equations ***(Faiz et al., 2023)***:

$$\mathbf{EE\%} = \frac{\mathbf{Weight\ of\ initial\ drug - Weight\ of\ free\ drug}}{\mathbf{Weight\ of\ initial\ drug}} \times \mathbf{100}$$

Particle morphology

Formulation morphology of REP-NLCs vesicles was observed visually via transmission electron microscope (TEM) (JEOL, JEM-1230, Tokyo, Japan) at 80 kilovolts (KV). Initially, samples of REP-NLCs were diluted with 1:200 double-distilled water and carried on a carbon-coated copper grid, and the samples were allowed to dry at room temperature overnight. The film on the grid was negatively stained by the addition of 2% uranyl acetate and left to dry at room temperature ***(Fouad et al., 2023)***. Then, the prepared samples were examined under TEM.

In-vitro release studies of RPG

In-vitro release tests were performed for pure Repaglinide, REP-NLC via dialysis bag technique using dialysis bags (MWCO 12-14KD, Sigma, USA) ***(Yaghoobian et al., 2020)***. Dialysis membrane was washed before use with distilled water to remove excess glycerin and Sulphur ***(Fouad et al., 2023)*** then soaked overnight in the release media (PBS) pH 6.8 + 0.5 % tween 20 to confirm more sink conditions of dissolution media. Two milligrams of pure REP and equivalent amount of the developed REP-NLC were suspended in 5 ml of the release medium into dialysis bag which was tightly closed from two sides by a thermo-resistant thread to avoid leaking and immersed in the Dissolution apparatus, (six-spindle dissolution tester, Pharma test, type PTWII, Germany) which contained 400 ml of the release medium at each vessel (75 ±1 rpm and 37±0.5 °C). At predetermined interval 5 mL samples were withdrawn and filtered via 0.220 μm syringe filter at specified time intervals (0.15, 0.30, 1, 2, 4, 6, 8, 10, 12, and 24 hours) and continuously replaced with equal volumes of fresh dissolution medium to maintain sink conditions ***(Ahmad et al., 2023)***. The aspirated samples were measured using a UV-Vis spectrophotometer at the calculated λ_{max} of REP (242 nm). All measurements were performed in triplicates (n=3) against blank.

RESULTS and DISCUSSION

Analytical method development for Repaglinide:

UV scanning of Repaglinide

The UV scan of REP exhibited absorption peaks at 242 nm in absolute methanol, which aligns with the λ_{max} of Repaglinide reported in scientific literature ***(Shaikh et al., 2020)***, as depicted in **Figure (1)**

Construction of calibration curve of REP in methanol

Figure (2A) shows the absorbance of REP after serial dilution (2.5–25 µg/ml) in methanol, which showed a linear relationship (R = 0.9992) between the absorbance obtained and REP concentrations, which indicated that the REP obeys Beer-Lambert´s law λ_{max} (242 nm).

Construction of calibration curve of REP in PBS (pH 6.8) + 0.5 % Tween 20

Figure (2B) showed the absorbance of REP after serial dilution (2.5 -25 µg/ml) in PBS pH 6.8 + 0.5% Tween 20 while, which showed a linear relationship (R=0.9992) between the absorbance obtained and REP concentrations which indicated that, the REP obeys Beer-Lambert law at λ_{max} (242 nm).

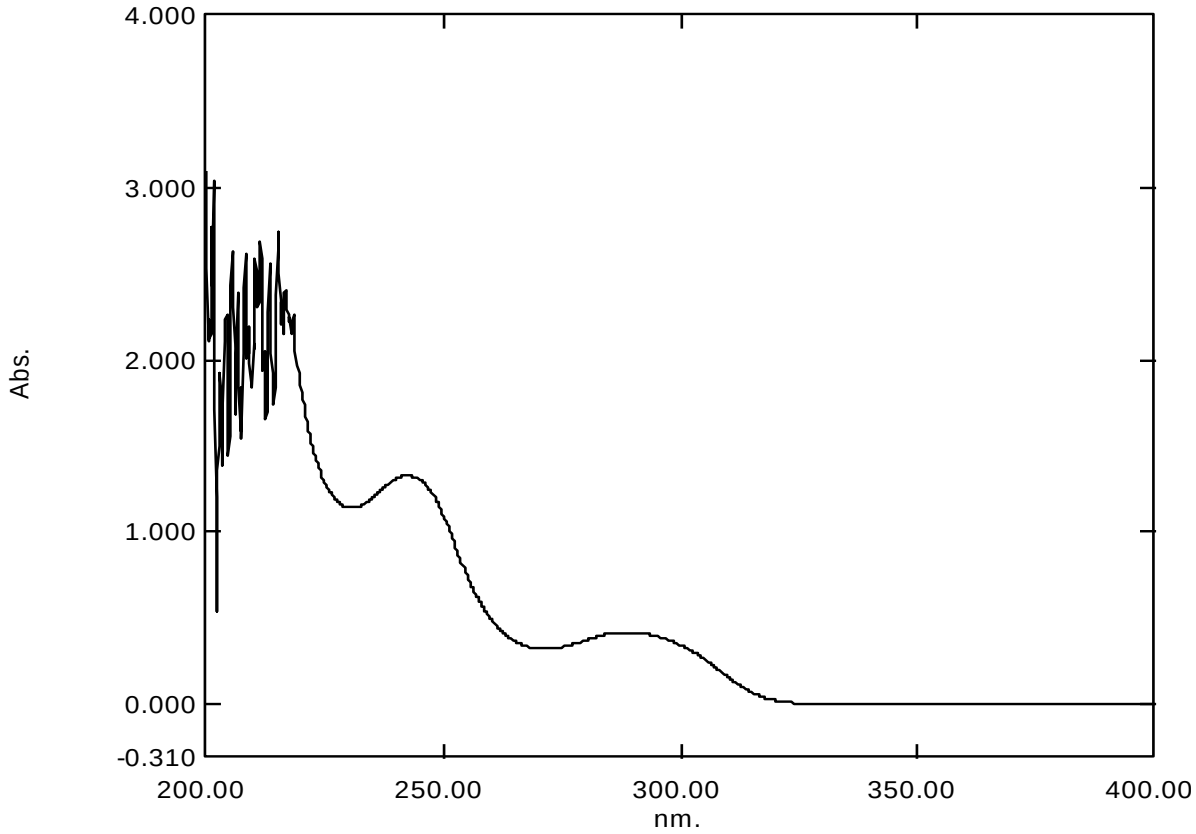

Figure (1): UV Scanning of Repaglinide in methanol

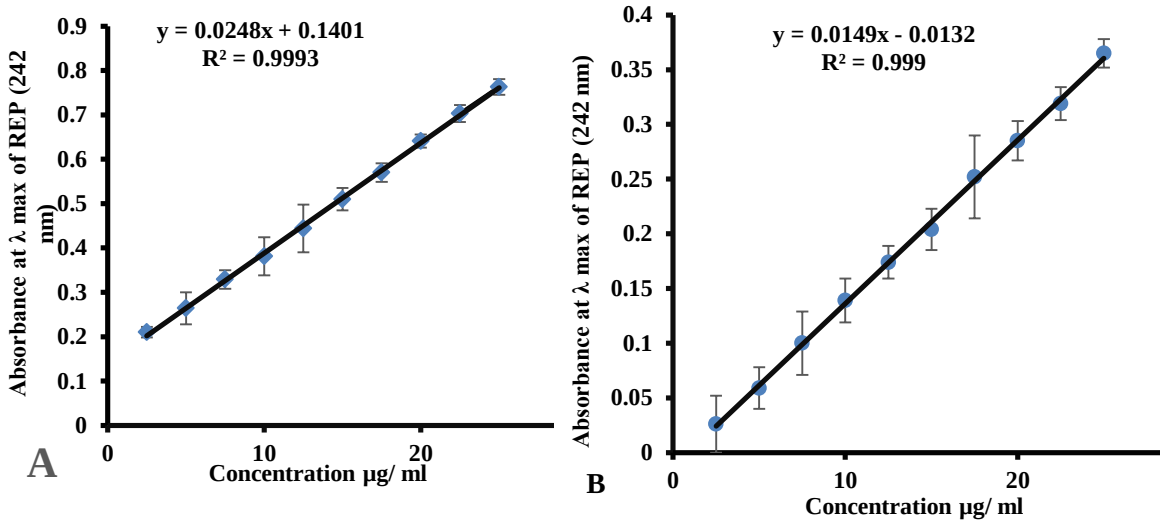

Figure (2): Standard calibration curve for REP in (A) methanol and (B) Phosphate buffer Ph 6.8 + 5% Tween 20 at λ_{max} of (242 nm)

Solubility analysis of Repaglinide in solids lipids

Since lipids are the primary components of LNPs, they exert a significant impact on the drug entrapment efficiency, stability, and sustained release characteristics of the formulations. The solubility was determined by assessing the visual clarity resulting from the addition of the drug to the molten lipid phase. The drug solubility within the solid lipid core primarily determines the ability of nanostructure lipid carrier (NLCs) formulations to tolerate a certain drug ***(Pandey et al., 2020)***. To maximize the E.E of the NLCs formulation, the solubility of REP in several solid lipids was assessed **Figure (3)**. This evaluation enabled us to identify a solid lipid that is appropriate for the preparation of the NLCs formulation. The experiments with solid lipids demonstrated that the affinity of REP to solid lipid was in order Precirol®ATO 5< Compritol®888ATO) < Cetyl alcohol < Gelucire®50/13 < Labrafil®M2130CS< Bees wax.

Precirol®ATO5 and Compritol®888ATO showed higher REP solubilizing ability, with solid lipid values per 100 mg of REP (w/w) of 800 ± 100 mg, 1600 ± 225 mg respectively. These results correlated with the imperfect matrix structure of Compritol®888ATO, Precirol®ATO 5, which are formed due to its chemical nature (mono-, di-, and triglyceride contents) and its composition that containing fatty acid of different chain length that impart loose, highly porous structural characteristics, which allows easier accommodation and higher solubility of the drug. High solubility characteristics of REP in Precirol®ATO 5 and Compritol®888ATO could be attributed to their low HLB values. The lower the HLB value, the more lipophilic the lipid is and in turn, the higher the HLB value, the more hydrophilic the lipid is. As a result, lipids with low HLB values are more favorable for solubility of hydrophobic REP than lipids with high HLB values. For the same reason, REP has low solubility in Gelucire®50/13 (HLB =13) and Cetyl alcohol (HLB =15.5) ***(Pandey et al., 2020)***. In this investigation, Precirol®ATO 5 and Compritol®888ATO were used as the lipid core for the creation of REP-NLCs based on the previous results.

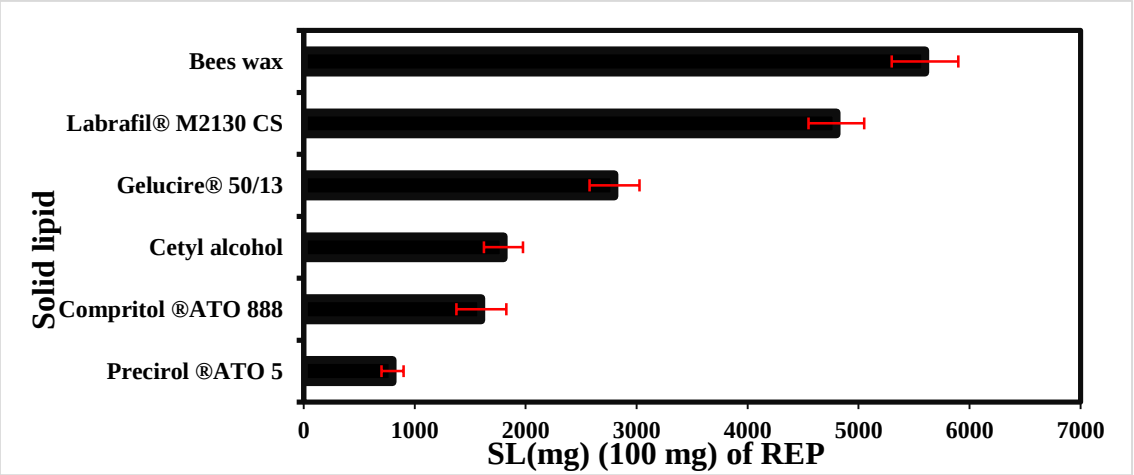

Figure (3): Histogram showing the solubility study of Repaglinide (REP) in different solid lipid

Solubility analysis of RPG in liquid lipids

Screening of liquid lipids was evaluated based on solubility of REP in different liquid lipids. Increased drug solubility in the oil phase reduces the need for surfactants, hence minimizing their harmful effects. The results of solubility for REP in different oils was depicted in **Figure (4)**, which clearly demonstrated that REP exhibited the greatest solubility in peppermint oil (33.36 ± 2.008 mg/ml), Capryol™90 (23.07±2.057 mg/ml) and Labrasol®ALF (14.37 ± 1.910 mg/ml). Medium-chain triglycerides are the preferred choice for lipid-based products because of their high affinity for lipophilic drugs, emulsification properties, enhance oral absorption of lipophilic drugs and lack of susceptibility to oxidation during long-term storage ***(Ansari et al., 2023)***.

The high solubility of (REP) in peppermint oil (33.36 ± 2.008 mg/ml) could be attributed to the complex composition of peppermint oil, which contains various alcohols, ketones, and terpenes (such as menthol, menthone, 1,8-cineole, methyl acetate, methofuran, isomenthone, limonene, b-pinene, a-pinene, and pulegone). These compounds may aid in the solubilization of REP by interacting with one or more of the different functional groups of REP, such as –NH and –C=O **(Anwar *et al.*, 2019)**.

The solubilization capacity of Capryol™90 (23.07 ± 2.057 mg/ml) and Labrasol®ALF (14.37 ± 1.910 mg/ml), for REP is due to their natural ability to form emulsions and their chemical composition (PEG-medium chain triglycerides). PEG/glyceride compounds are known to have a higher capability to encapsulate a wide range of lipophilic and hydrophilic drug molecules within lipids. Moreover, the solubility of the drug was affected by the concentration of Caprylic acid (C8) in the oils. Oils with a larger amount of Caprylic acid (namely, Labrasol®ALF and Capryol™90 with Caprylic acid contents of 80% and 90% respectively) exhibited greater solubility. This behavior can be explained by the polarity of Caprylic acid, which makes it more effective in dissolving drugs that are not easily soluble in water. Therefore, Labrasol®ALF, and Capryol™90 were chosen as liquid lipids for further study due to their high solubilizing capacity for REP. Peppermint oil was excluded from

consideration because of its flash point (66.1°C) was lower than the temperature required for formulation preparation ***(El-Gendy et al., 2020)***.

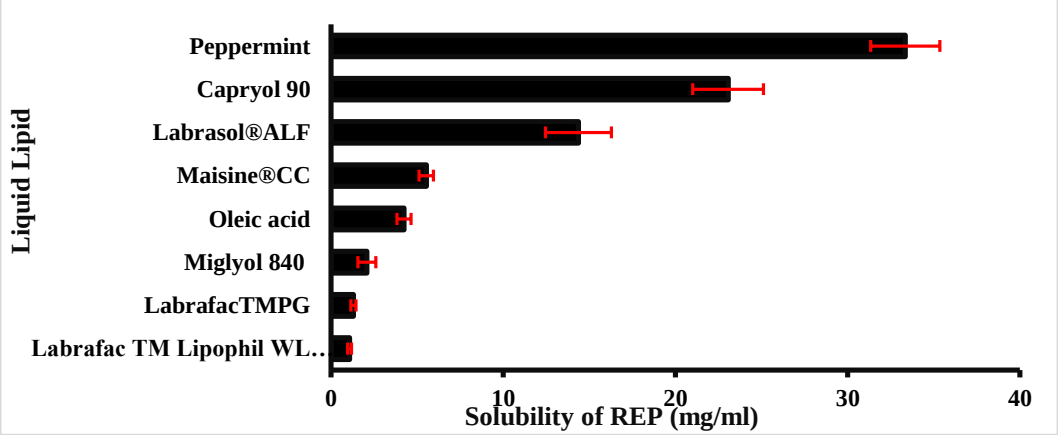

Figure (4): Histogram showing the solubility study of Repaglinide (REP) in different liquid lipid

Physical compatibilities between solid lipids and liquid lipids

The physical compatibility of two specific solid lipids (Precirol®ATO5 and Compritol®888ATO) with two specific liquid lipids (Capryol™90, and Labrasol®ALF) was assessed using visual and filter paper evaluation and the results obtained are presented in **Table (1)**, which revealed that the mixtures of (Precirol®ATO 5 - Capryol™90), (Compritol®888ATO - Labrasol®ALF) and (Compritol®888ATO - Capryol™90) exhibited phase separation and the presence of oil droplets residue on the filter paper, indicating the creation of non-uniform mixtures. This observation can be attributed to the reduction in the aggregate melting temperature of the lipid mixes. However, there were not any residues of oil droplets on the filter paper from the combination of (Precirol®ATO5 and Labrasol®ALF) ***(Sartaj et al., 2022)***. Thus, the solid and liquid lipids (Precirol®ATO5 - Labrasol®ALF) were chosen for further exploration due to their solubility and affinity for REP, as well as their physical compatibility.

Table (1): Physical Compatibilities between solid lipids and liquid lipids

Solid lipids	Liquid lipids	Compatibility using visual examination	Compatibility usingfilter paper
Precirol®ATO5	Capryol™90	Compatible	Incompatible
	Labrasol®ALF	Compatible	Compatible
Compritol®888ATO	Capryol™90	Compatible	Incompatible
	Labrasol®ALF	Compatible	Incompatible

Selection of a binary lipid phase ratio

Solid-liquid lipid proportion was chosen with the goal of having enough drug solubility with a legitimate liquefying point to maintain the solid/semisolid consistency of the particles at room temperature. It was seen that the solid-liquid lipid blend in the proportion up to 70:30 had an adequate melting point (55–59 °C), as recorded in **Table (2)**. Furthermore, an increase in liquid lipid content, the melting point of the blends was below the ideal level. Consequently, 70:30 was chosen as the working ratio for the solid-liquid lipid mixture in all NLC formulations. In addition, 70:30 is the most appropriate, common, and widely applied by most previous related studies ***(Scioli Montoto et al., 2020)***.

Table (2): Determination of the SL: LL ratios of solid lipid and liquid lipid mixture using melting point technique

SL: LL combination	Ratio of SL: LL	Melting point (°C)
Precirol®ATO 5: Labrasol®ALF	90: 10	65.2
	80:20	64
	70: 30	63.5
	60: 40	62.5
	50: 50	58
	40:60	43
	30:70	40

Screening study of surfactants: assessment of dispersion properties

The emulsification capacity and stability of the emulsion were regarded as parameters for the surfactant selection. A greater degree of transmittance is associated with smaller particles, resulting in improved emulsification **(Vieira et al., 2020)**. The most proper (HLB) value for the manufacture of stable O/W emulsion lies between 12 and 16 ***(Abd El-Halim et al., 2020)***. As depicted in **Table (3)**, results revealed that Poloxamer®188, Poloxamer®407, Cremophor®RH40, Cremophor®EL and Tween®20 showed maximal emulsification capacity for binary lipids of the selected lipid mixture (Precirol®ATO5 - Labrasol®ALF), which showed higher % Transmittance for these surfactants. On the other hand, the binary selected lipid mixture mentioned above exhibited poor emulsification and formed turbid nanoemulsions with Span®80 and Span®20 where % Transmittance for these surfactants was low due to their low HLB. Using a surfactant with a higher (HLB) led to the creation of vesicles with smaller diameters and a high percentage of light transmission ***(Subramaniam et al., 2020).***

Screening study of surfactant combinations: assessment of dispersion properties

Previous literature has clearly shown that the kind and amount of surfactant has a significant impact on the size of nanoparticles and stability. The surfactant quantity should be sufficient to fully coat the hydrophobic nanoparticles, therefore reducing their interfacial tension and inhibiting the merging of the oily droplets in the nanoemulsion. The synergy resulting from the combination of two or more surfactant, resulting in the formation of nanoparticles with small dimensions and a suitable viscosity that ensures long-term storage stability. In this study, the surfactant ratio of 1:1 showed excellent

emulsification capacity and enhanced the stability of nanoemulsions formed by the combination of lipids. Moreover, these nanoemulsions exhibited greater levels of transmittance as seen in **Table (4)**. The observed outcomes can be ascribed to the same factors discussed earlier in the context of the surfactant screening study ***(Kovačević et al., 2020)***.

Table (3): Miscibility study of Precirol®ATO 5 and Labrasol®ALF binary lipid mixture with different surfactants

SL: LL in ratio	SAA 10 ml of 5% solution	% Transmittance ± SD
Precirol®ATO 5: **Labrasol®ALF**	Poloxamer®188	98.36 ± 2.2
	Cremophor®RH	97.45 ± 4.3
	Tween®20	96.285 ± 3.6
	Poloxamer®407	95.20 ± 5.5
	Cremophor®EL	94.13 ± 6.1
	Span®20	15.88 ± 4.9
	Span®80	9.19± 2.9

Table (4): Miscibility study of Precirol®ATO 5 and Labrasol®ALF binary lipid mixture with combinations of different surfactants

SL: LL in ratio	SAA Combination (1:1)10 ml of 5 % solution	%Transmittance ± SD
Precirol®ATO5: **Labrasol®ALF**	Tween®20: Cremophor®EL	98.6 ± 3.9
	Tween®20: Cremophor®RH	97.1 ± 1.3
	Poloxamer®407: Cremophor®EL	85.75 ± 6.3
	Poloxamer®188: Cremophor®RH	94.2 ± 6.9
	Poloxamer®188: Tween®20	98.5 ± 2.8

Hence, based on the introduction and demulsification study of surfactants (Poloxamer®407, Poloxamer®188, Cremophor®EL, Cremophor®RH40 and Tween®20) were selected as surfactants alone or in combination at ratio (1:1) for every binary lipid mixture for the preparation of NLCs.

Fabrication of Repaglinide nanostructured lipid carriers (REP-NLC)

Based on screening and solubility studies, NLC formulations were developed and enhanced utilizing a lipid phase consisting of Precirol®ATO 5 and Labrasol®ALF. These lipids were selected based on their solubility for REP, as determined through screening and solubility tests. The surfactants used in this study were Poloxamer®407, Poloxamer®188, Cremophor®EL, Cremophor®RH and Tween 20. The lipid phase to surfactant concentration remained constant at 4% (w/w) and 2.5% (w/w), respectively. The concentration of REP was kept at 5% (w/w) of the lipid phase, the lipid phase should not exceed 5 % w/w, where the particle size increases as the concentration of solid lipid increases, which is attributed to the higher viscosity **(Sakellari et al., 2021)**. As formulations were designed to be orally used, surfactants have been established at a pleasant 2.5% concentration (w/w). The synergistic effect of the surfactant combination was observed to be superior to the individual effects due to the combined impact of two surfactants **(Onugwu et al., 2022)**.The formulation composition was provided in **Table (5)**. The preparation of REP-NLCs involved the use of homogenization followed by

probe sonication technique to decrease particle size and inhibit crystal growth and agglomeration ***(Putri et al., 2020)***. Furthermore, additional physical characterization of each formulation is necessary to determine the most suitable one for further investigations. The small particle size and high negative zeta potential values of NLCs indicate the stability of the formed colloidal dispersion.

Table (5): Suggested formulae of REP-NLCs using Precirol®ATO 5 and Labrasol®ALF

F. N	SL (70%) (4%) of Total Formula (g)	LL (30%) (4%) of Total Formula (g)	SAA (2.5%) of Total Formula (g)						Drug (5%) of Lipids (mg)	Water (93.3%) (g)
	Perciro l®ATO 5	Labraso l®ALF	L.F6 8	L.F127	Cr. RH	Cr. EL	T.2 0	T.80	REP	
F1	2.8	1.2	1.25		1.25				200	93.3
F2	2.8	1.2					2.5		200	93.3
F3	2.8	1.2		1.25	1.25				200	93.3
F4	2.8	1.2				2.5			200	93.3
F5	2.8	1.2				1.25	1.25		200	93.3
F6	2.8	1.2			2.5				200	93.3

Where SL = Solid lipid, LL = Liquid lipid, SAA = Surface active agent, P =Precirol®ATO 5, LB = Labrasol®ALF, L F68 = Lutrol®F68, L F127 = Lutrol®F127, Cr RH = Cremophor®RH40, Cr EL = Cremophor®EL, T.20=Tween 20 and REP = Repaglinide

Physicochemical characterization of REP-NLC formulations

Particle size

As represented in **Table (6)** and **Figure (5A)** the observations revealed that all the designed formulations were in the colloidal nanometer range (<898.4 nm). Particle size of REP-NLCs, nanoparticles ranged from (59.1±3.2 to 898.4±40.3nm). The results clearly indicate that formulations containing multiple surfactants yield smaller particle sizes compared to those containing only one surfactant, as shown in **Table (6)** (F1, F3). All these formulations exhibit smaller particle sizes respectively (59.1±3.2, 150.7±5.1) due to the synergistic effect of combining two surfactants to form blended surfactant films on the particles. While formulae (F2, F4, F6) have larger particle sizes (234.7±1.8, 898.4±40.3, 373.3±5), because they include just one surfactant. This single surfactant is not enough to effectively cover the particle surfaces and produce nanoparticles with small sizes ***(Anwar et al., 2019)***. Moreover formula (F5) has a particle size 569.2±33.9, because of the viscous nature of Cremophor®EL, increase in its content will also contribute to the increased viscosity of formulations. The hydrophilicity of the surfactant head group also contributes to reducing the size of the vesicles, which could be linked to the smaller hydrophobic core **(Bnyan et al., 2019)**. Typically, it is

recommended to a particle with size smaller than 300 nm is efficient for intestinal transport which makes absorption easier ***(Jiang et al., 2022)***.

Polydispersity index

PDI is employed to assess the average uniformity of particle size. Higher PDI values suggest a greater degree of variation in the size distribution of the particle sample. The acceptable range for PDI lies between 0.08 to 0.7 as illustrated in **Table (6)** and **Figure (5B)**. The NLC dispersions that were prepared had a PDI value of < 0.781± 0.139, which was obtained via the chosen preparation process. This result indicated that the NLCs have a uniform and narrow size distribution. Furthermore, this PDI value falls within the allowed range of 0.08-0.7 for PDI. The same rationale has been documented by ***(Hamishehkar et al., 2018)***.

Zeta potential measurement

The Zeta potential values for all the formulated designs are reported in **Table (6)** and depicted in **Figure (5C)**. The results indicated that the different formulations had a consistently negative surface charge, and this negative charge effectively prevented particle aggregation. This negative charge was ascribed to the anionic properties of the lipid, or due to the presence of non-ionic surfactants , which often confer a negative charge to particles on which they are adsorbed ***(Al-mahallawi et al., 2021)***. The ZP values of all formulations range from -32.27±1.01 to -28.87±1.59 mV. The use of Poloxamer 188 and Poloxamer 407 in NLC formulations have been found to enhance the zeta potential of the nanoparticles, resulting in enhanced physical stability of the system ***(Sathyanaryana and Sudheer, 2022)***. Zeta potential value equal to or greater than 30 mV can be considered as an indication of physical stable. This is because the electrostatic repulsion forces outweigh the Vander Waals forces, as explained by ***(Ambhore et al., 2016)***. The nonionic surfactant utilized in this investigation exhibits superior steric stabilization and inferior electrostatic stabilization, resulting in the formation of a well-formed coating over the particles of REP-NLCs.

Entrapment efficiency

Repaglinide exhibits low solubility in water, resulting in a reduced ability to escape from lipid carriers. Consequently, it demonstrates high entrapment efficiency, as lipophilic active ingredients are effectively trapped within the core of NLC. The entrapment efficiencies of all developed nanostructured lipid carriers (NLCs) are reported in **Table (6)** and illustrated in **Figure (5D)**. The encapsulation efficiencies ranged from 85.32 ± 4.6 % to 70.11 ± 5.3%. The high entrapment efficiency of REP in NLCs can be attributed to its high lipophilic nature (log p ~ 4.2) **(Soni et al., 2020)**.

The EE showed an increase by ascending the particle size from the smallest size F1 (57.1 nm, 80.73 %) to size F3(150.7 nm, 85.32%). However, more increase in particle size resulted in a drop in EE, as observed in F4 and F5 (898.4 nm, with EE 74.96 %), (569.2 nm, with EE 77.93%) respectively. Reducing the size of the particles enhances the specific surface area, resulting in an increase in EE. On the other hand, a greater decrease in particle size results in a larger surface area, which in turn increases

the mobility and tendency of the drug to escape from the carrier leading to decrease in EE as in F1 (Poloxamer188 + Cremophor®RH40) NLCs, due to it restricts the amount of active substances that may be entrapped ***(Eh Suk et al., 2020)***.

Regarding the type of surfactant, it was clearly observed that NLCs formulation prepared using poloxamer®188 and poloxamer®407 in combination with other surfactant (F1, F3) have higher % EE (80.73±5.2, 85.32±4.6) respectively than that prepared using other surfactants without poloxamer (F2, F4, F5, F6) have lower % EE (76.48±5.3, 74.96±5.6, 77.93±4.2, 70.11±5.3) respectively. This fact might be attributed to the high value of HLB of poloxamer®188 (HLB ~ 29) and poloxamer®407 (HLB ~ 18 - 23) compared to other surfactants. Where poloxamer®188 and poloxamer®407 in prepared formulation act as steric through creating an effective coat on the surface of NLCs which subsequently prevents REP leakage to the external phase and thus retain high concentration of REP inside lipid nanoparticles ***(Xinying et al., 2023)***.

Furthermore, the entrapment efficiency of formulations containing a combination of two surfactants have higher entrapment efficiency than formulations containing a single surfactant (F2, F4, F6) have low EE (76.48%, 74.96%, and 70.11% respectively). This is due to the synergistic effect of co-absorbing different types of surfactants, resulting in the production of smaller nanoparticles with improved stability. Also, F6 formula, which utilizes Cremophor RH40 as a sole surfactant, exhibits a low percentage of encapsulation efficiency (70.11±5.3) %.

Table (6): Particle size, polydispersity indices, zeta potential and entrapment efficiency of REP-NLCs formulations.

F. N	PS (nm)	PDI	ZP (mV)	EE (%)
F1	59.1±3.2	0.328±0.037	−29.83±0.51	80.73±5.2
F2	234.7±1.8	0.291±0.017	−30.43±0.32	76.48±5.3
F3	150.7±5.1	0.426±0.05	−32.27±1.01	85.32±4.6
F4	898.4±40.3	0.781±0.139	−28.87±1.59	74.96±5.6
F5	569.2±33.9	0.519±0.035	−28.97±2.49	77.93±4.2
F6	373.3±5.0	0.482±0.053	−26.13±7.37	70.11±5.3

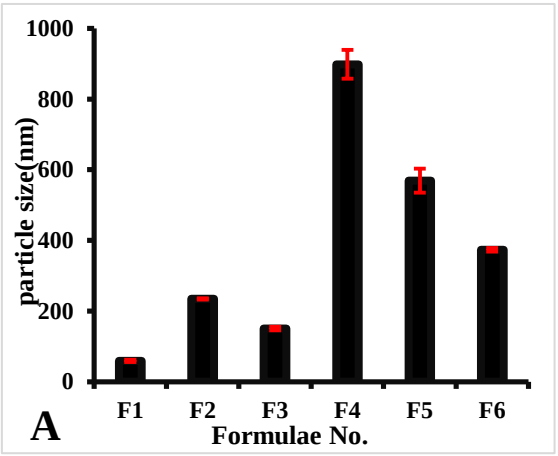

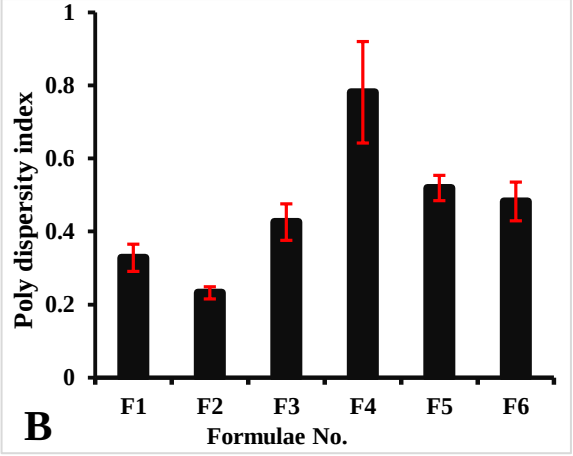

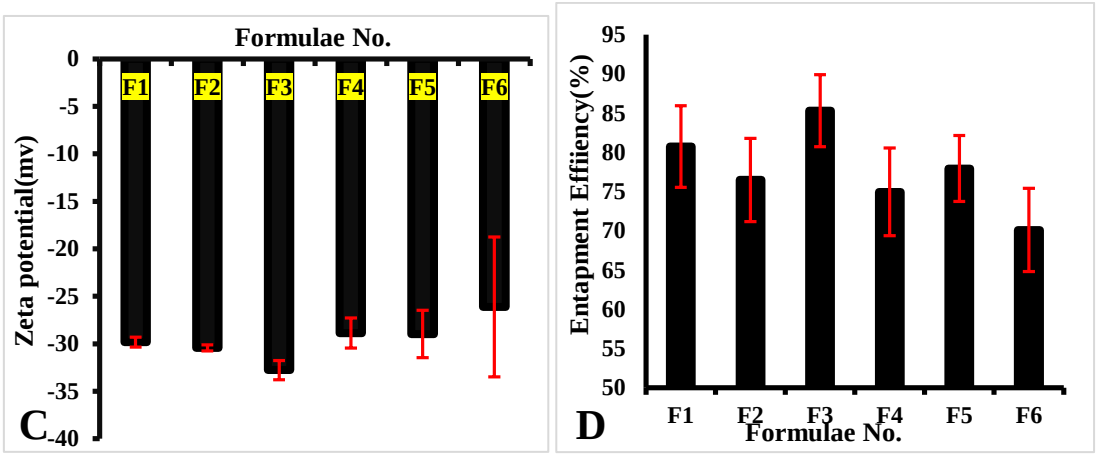

Figure (5): Histogram showing (A) the mean PS, (B) PDI, (C) ZP and (D) %EE of REP-NLCs formulations

Rank order for the different formulations of REP-NLCs

As appeared in **Table (7)** The rank order was performed for all prepared NLCs formulations (F1 to F6) in order to choose the best formula based on the previous measured characterization as Particle size (PS), polydispersity index (PDI), zeta potential (ZP), and encapsulation efficiency of REP-NLCs where the formulae F3 was chosen as the best formula for further investigations and illustrated in **Figure (6)** which consisted of Precirol®ATO as the solid lipid, Labrasol®ALF as the liquid lipid, and a surfactant blend of poloxamer 407 and Cremophor RH40 (1:1).

Table (7): Rank order of REP-NLCs formulations

F. N	PS	PDI	ZP	% EE	TOTAL	R.O.
F1	1	2	3	2	8	2
F2	3	1	2	4	10	3
F3	2	3	1	1	7	1
F4	5	5	4	3	21	5
F5	6	6	5	5	18	4
F6	4	4	6	6	20	6

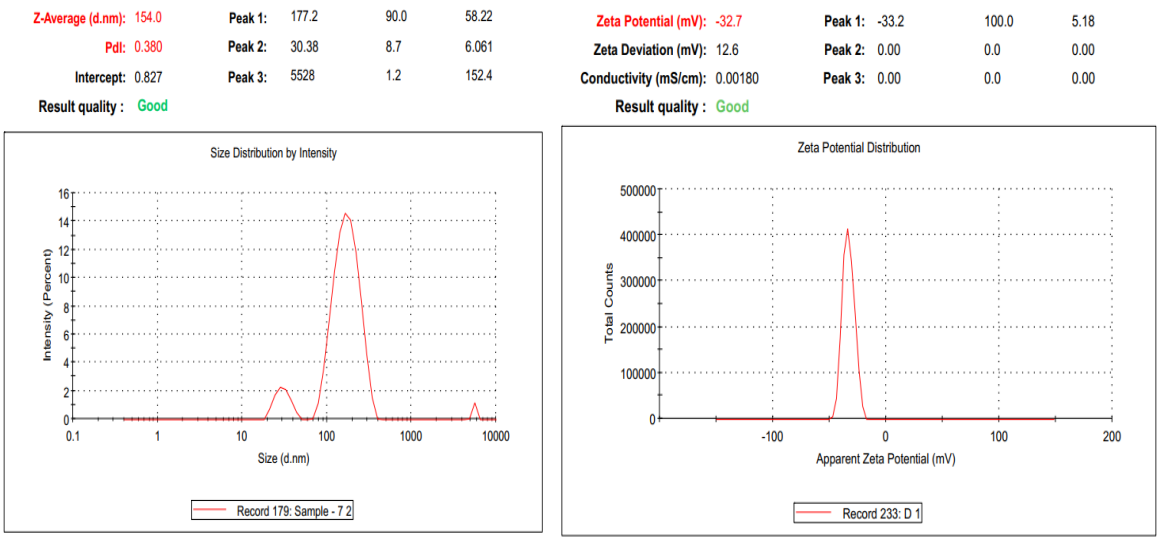

A **B**

Figure (6): (A) Particle size of the best formulae taken from three charts and (B) Zeta potential of the best formulae taken from three charts.

Particle Morphology

The morphology of freshly prepared REP-NLCs samples were observed using a transmission electron microscope (TEM) with a magnification of 20,000 times. The image clearly demonstrates that the NLC vesicles exist as distinct entities. All particles depicted in the photograph were inside the nanometer scale. The transmission electron microscopy (TEM) analysis demonstrated that the nanoparticles in the RPG-NLC formulation exhibited a uniform ellipsoidal or spherical morphology, as depicted in **Figure (7)**. This might indicate homogeneity and good uniformity of the release of the entrapped REP ***(Al-mahallawi et al., 2021)***. The vesicles appear smaller when measured using TEM compared to DLS due to the drying process involved in preparing the TEM sample. This causes the nanoparticles to shrink, resulting in a smaller size compared to the DLS measurement. Where in DLS, the hydration of the samples maintains the size of the nanoparticles ***(Elkarray et al., 2022).***

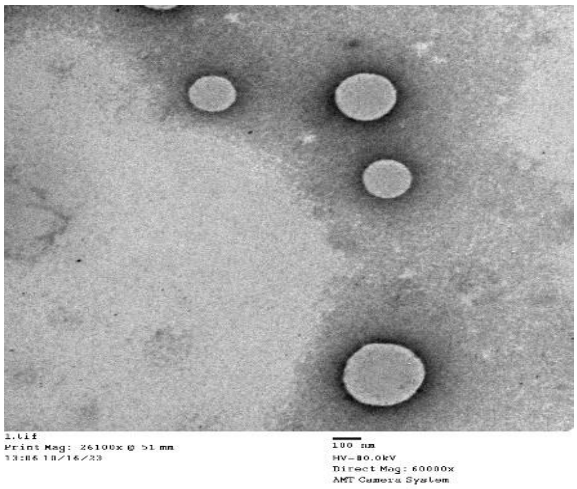

Figure (7): TEM image REP-NLCs

In-vitro Release Studies of Repaglinide

The graph in **Figure (8)** displays the relationship between the cumulative drug release percentage and time. In the case of batch-I, the release of REP was rapid, with approximately 98 ± 1.6 % of REP being released within the first 4 hours. On the other hand, batch-II exhibited sustained drug release profiles 100 ± 8.2% of the drug being released within 24 hours. One notable feature of the release diagram of NLCs was its biphasic profile. It exhibited an initial burst effect within the first 4 hours, releasing approximately 43% of REP. This was followed by a sustained release over a period of 24 hours, releasing almost all the drug remained ***(Dasineh et al., 2021)***. The REP-NLCs had a biphasic release pattern, characterized by an initial rapid release followed by a steady release over a 24-hour period, as shown in **Table (8)**. The initial fast release of REP from REP-NLCs was found to be 33.75± 5.2 % (2 h). Lipid nanoparticles often exhibit a high burst release, as observed in the study conducted by **(Shazly, 2017)**. The subsequent controlled release was attained from REP-NLCs (100 ± 8.2%) within a 24-hour period.

The sustained release that occurs after the burst release may be attributed to the liberation of REP from the lipid core matrix of NLCs through the process of matrix erosion or degradation **(Sharma et al., 2023)**. Sustained release drug delivery system is very imperative, as it would permit for an extended residence of the drug at the outside of the release site which would increase the drug bioavailability and extending the favourite beneficial effect. The dual release behavior is ideal for in-vivo absorption, the initial burst release of REP at the first 2 hours allows effective concentration of the drug rapidly in plasma producing promoted antidiabetic effect, while the following sustained release pattern can maintain the therapeutic concentration within the therapeutic range in plasma for prolonged periods reducing the unwanted reported complaints of toxicity or underexposure **(Kelte Filho et al., 2021)**.

Table (8): % Cumulative release of REP from Pure REP suspension (0.5%Na CMC), REP-NLCs formulations in PBS (pH 6.8) with adding Tween 20 (0.5% w/v)

Time	Pure REP suspension		REP-NLCs	
	average	±SD	average	±SD
hours				
0.00	0	0	0	0
0.15	20.52	2.6	11.29	1.2
0.30	34.87	4.6	22.57	4.3
1.00	52.25	5.8	26.11	3.9
2.00	78.33	6.4	33.75	5.2
4.00	100.00	8.4	43.75	4.9
6.00			63.43	3.8
8.00			78.11	6.9
10.00			86.77	5.6
12.00			93.09	4.8
24.00			100.00	8.2

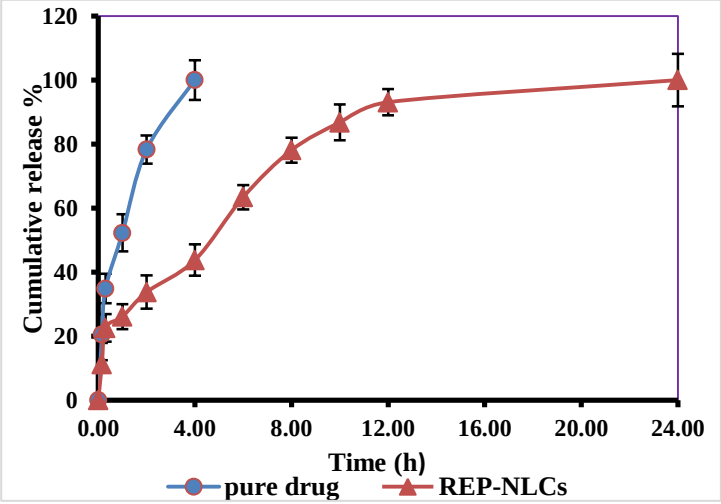

Figure (8): % Cumulative release of REP from Pure REP suspension (0.5%Na CMC) and REP-NLCs formulations in (PBS) pH 6.8 +0.5% Tween 20

REFERENCES

Abd El-Halim, S.M., Abdelbary, G.A., Amin, M.M., Zakaria, M.Y., Shamsel-Din, H.A., and Ibrahim, A.B. (2020). Stabilized oral nanostructured lipid carriers of Adefovir Dipivoxil as a potential liver targeting: Estimation of liver function panel and uptake following intravenous injection of radioiodinated indicator. DARU Journal of Pharmaceutical Sciences *28*, 517-532.

Ahmad, M., Khan, S., Shah, S.M.H., Zahoor, M., Hussain, Z., Hussain, H., Shah, S.W.A., Ullah, R., and Alotaibi, A. (2023). Formulation and Optimization of Repaglinide Nanoparticles Using Microfluidics for Enhanced Bioavailability and Management of Diabetes. Biomedicines *11*, 1064.

Akel, H., Ismail, R., Katona, G., Sabir, F., Ambrus, R., and Csóka, I. (2021). A comparison study of lipid and polymeric nanoparticles in the nasal delivery of meloxicam: Formulation, characterization, and in vitro evaluation. International Journal of Pharmaceutics *604*, 120724.

Al-mahallawi, A.M., Ahmed, D., Hassan, M., and El-Setouhy, D.A. (2021). Enhanced ocular delivery of clotrimazole via loading into mucoadhesive microemulsion system: In vitro characterization and in vivo assessment. Journal of Drug Delivery Science and Technology *64*, 102561.

Ambhore, N.P., Dandagi, P.M., and Gadad, A.P. (2016). Formulation and comparative evaluation of HPMC and water soluble chitosan-based sparfloxacin nanosuspension for ophthalmic delivery. Drug delivery and translational research *6*, 48-56.

Ansari, M.M., Vo, D.-K., Choi, H.-I., Ryu, J.-S., Bae, Y., Bukhari, N.I., Zeb, A., Kim, J.-K., and Maeng, H.-J. (2023). Formulation and Evaluation of a Self-Microemulsifying Drug Delivery System of Raloxifene with Improved Solubility and Oral Bioavailability. Pharmaceutics *15*, 2073.

Anwar, W., Dawaba, H.M., Afouna, M.I., and Samy, A.M. (2019). Screening study for formulation variables in preparation and characterization of candesartan cilexetil loaded nanostructured lipid carriers. Pharm. Res *4*, 8-19.

Bnyan, R., Khan, I., Ehtezazi, T., Saleem, I., Gordon, S., O'Neill, F., and Roberts, M. (2019). Formulation and optimisation of novel transfersomes for sustained release of local anaesthetic. Journal of Pharmacy and Pharmacology *71*, 1508-1519.

Dash, S.K., Patra, C.N., Acharjya, S.K., Jena, G.K., Panigrahi, K.C., Kumar, N.K., and Das, P.S. (2022). Development and Characterization of Paliperidone Loaded Nanostructured Lipid Carrier. INDIAN JOURNAL OF PHARMACEUTICAL EDUCATION AND RESEARCH *56*, 1003-1012.

Dasineh, S., Akbarian, M., Ebrahimi, H.A., and Behbudi, G. (2021). Tacrolimus-loaded chitosan-coated nanostructured lipid carriers: preparation, optimization and physicochemical characterization. Applied Nanoscience *11*, 1169-1181.

Ebrahimi, H.A., Javadzadeh, Y., Hamidi, M., and Jalali, M.B. (2015). Repaglinide-loaded solid lipid nanoparticles: effect of using different surfactants/stabilizers on physicochemical properties of nanoparticles. DARU Journal of Pharmaceutical Sciences *23*, 1-11.

Eh Suk, V.R., Mohd. Latif, F., Teo, Y.Y., and Misran, M. (2020). Development of nanostructured lipid carrier (NLC) assisted with polysorbate nonionic surfactants as a carrier for l-ascorbic acid and Gold Tri. E 30. Journal of food science and technology *57*, 3259-3266.

El-Gendy, M.A., Mansour, M., El-Assal, M.I., Ishak, R.A., and Mortada, N.D. (2020). Delineating penetration enhancer-enriched liquid crystalline nanostructures as novel platforms for improved ophthalmic delivery. International Journal of Pharmaceutics *582*, 119313.

Elkarray, S.M., Farid, R.M., Abd-Alhaseeb, M.M., Omran, G.A., and Habib, D.A. (2022). Intranasal repaglinide-solid lipid nanoparticles integrated in situ gel outperform conventional oral route in hypoglycemic activity. Journal of Drug Delivery Science and Technology *68*, 103086.

Faiz, S., Arshad, S., Kamal, Y., Imran, S., Asim, M.H., Mahmood, A., Inam, S., Irfan, H.M., and Riaz, H. (2023). Pioglitazone-loaded nanostructured lipid carriers: In-vitro and in-vivo evaluation for improved bioavailability. Journal of Drug Delivery Science and Technology *79*, 104041.

Fouad, S.A., Teaima, M.H., Gebril, M.I., Abd Allah, F.I., El-Nabarawi, M.A., and Elhabal, S.F. (2023). Formulation of novel niosomal repaglinide chewable tablets using coprocessed excipients: in vitro characterization, optimization and enhanced hypoglycemic activity in rats. Drug Delivery *30*, 2181747.

Hamishehkar, H., Bahadori, M.B., Vandghanooni, S., Eskandani, M., Nakhlband, A., and Eskandani, M. (2018). Preparation, characterization and anti-proliferative effects of sclareol-loaded solid lipid nanoparticles on A549 human lung epithelial cancer cells. Journal of Drug Delivery Science and Technology *45*, 272-280.

Jiang, X.-C., Zhang, T., and Gao, J.-Q. (2022). The in vivo fate and targeting engineering of crossover vesicle-based gene delivery system. Advanced drug delivery reviews *187*, 114324.

Kelte Filho, I., Machado, C.S., Diedrich, C., Karam, T.K., Nakamura, C.V., Khalil, N.M., and Mainardes, R.M. (2021). Optimized chitosan-coated gliadin nanoparticles improved the hesperidin cytotoxicity over tumor cells. Brazilian Archives of Biology and Technology *64*.

Kesharwani, R., Patel, D.K., and Yadav, P.K. (2022). Bioavailability enhancement of repaglinide using nano lipid carrier: Preparation characterization and in vivo evaluation. Int. J. Appl. Pharm. *14*, 181-189.

Kovačević, A.B., Müller, R.H., and Keck, C.M. (2020). Formulation development of lipid nanoparticles: Improved lipid screening and development of tacrolimus loaded nanostructured lipid carriers (NLC). International Journal of Pharmaceutics *576*, 118918.

Luo, Q., Yang, J., Xu, H., Shi, J., Liang, Z., Zhang, R., Lu, P., Pu, G., Zhao, N., and Zhang, J. (2022). Sorafenib-loaded nanostructured lipid carriers for topical ocular therapy of corneal neovascularization: development, in-vitro and in vivo study. Drug Delivery *29*, 837-855.

Mathur, P., Sharma, S., Rawal, S., Patel, B., and Patel, M.M. (2020). Fabrication, optimization, and in vitro evaluation of docetaxel-loaded nanostructured lipid carriers for improved anticancer activity. Journal of liposome research *30*, 182-196.

Onugwu, A.L., Attama, A.A., Nnamani, P.O., Onugwu, S.O., Onuigbo, E.B., and Khutoryanskiy, V.V. (2022). Development and optimization of solid lipid nanoparticles coated with chitosan and poly (2-ethyl-2-oxazoline) for ocular drug delivery of ciprofloxacin. Journal of Drug Delivery Science and Technology *74*, 103527.

Pandey, S.S., Patel, M.A., Desai, D.T., Patel, H.P., Gupta, A.R., Joshi, S.V., Shah, D.O., and Maulvi, F.A. (2020). Bioavailability enhancement of repaglinide from transdermally applied nanostructured lipid carrier gel: optimization, in vitro and in vivo studies. Journal of Drug Delivery Science and Technology *57*, 101731.

Putri, N.R.E., Firdausi, S.I., Najmina, M., Amelia, S., Timotius, D., Kusumastuti, Y., and Petrus, H. (2020). Effect of sonication time and particle size for synthesis of magnetic nanoparticle from local iron sand. J. Eng. Sci. Technol *15*, 894-904.

Rahman, M.A., Ali, A., Rahamathulla, M., Salam, S., Hani, U., Wahab, S., Warsi, M.H., Yusuf, M., Ali, A., and Mittal, V. (2023). Fabrication of sustained release curcumin-loaded solid lipid nanoparticles (cur-SLNs) as a potential drug delivery system for the treatment of lung cancer: Optimization of formulation and in vitro biological evaluation. Polymers *15*, 542.

Sakellari, G.I., Zafeiri, I., Batchelor, H., and Spyropoulos, F. (2021). Formulation design, production and characterisation of solid lipid nanoparticles (SLN) and nanostructured lipid carriers (NLC) for the encapsulation of a model hydrophobic active. Food Hydrocolloids for Health *1*, 100024.

Sartaj, A., Biswas, L., Verma, A.K., Sahoo, P., Baboota, S., and Ali, J. (2022). Ribociclib nanostructured lipid carrier aimed for breast cancer: Formulation optimization, attenuating in vitro specification, and in vivo scrutinization. BioMed Research International *2022*.

Sathyanaryana, T., and Sudheer, P. (2022). NANOSTRUCTURED LIPID CARRIERS: A NOVEL STRATEGY FOR TRANSDERMAL DRUG DELIVERY SYSTEMS. Indian Drugs *59*.

Scioli Montoto, S., Muraca, G., and Ruiz, M.E. (2020). Solid lipid nanoparticles for drug delivery: pharmacological and biopharmaceutical aspects. Frontiers in molecular biosciences *7*, 319.

Shaikh, N.K., Jat, R., and Bhangale, J.O. (2020). Development and Validation of Stability Indicating RP-HPLC and UV Method for Simultaneous Quantitation

of Repaglinide and Sitagliptin Phosphate in Combination. American Journal of PharmTech Research *10*, 95-114.

Sharma, D.S., Wadhwa, S., Gulati, M., Kumar, B., Chitranshi, N., Gupta, V.K., Alrouji, M., Alhajlah, S., AlOmeir, O., and Vishwas, S. (2023). Chitosan modified 5-fluorouracil nanostructured lipid carriers for treatment of diabetic retinopathy in rats: A new dimension to an anticancer drug. International journal of biological macromolecules *224*, 810-830.

Shazly, G.A. (2017). Ciprofloxacin controlled-solid lipid nanoparticles: characterization, in vitro release, and antibacterial activity assessment. BioMed research international *2017*.

Soni, N.K., Sonali, L., Singh, A., Mangla, B., Neupane, Y.R., and Kohli, K. (2020). Nanostructured lipid carrier potentiated oral delivery of raloxifene for breast cancer treatment. Nanotechnology *31*, 475101.

Subramaniam, B., Siddik, Z.H., and Nagoor, N.H. (2020). Optimization of nanostructured lipid carriers: Understanding the types, designs, and parameters in the process of formulations. Journal of nanoparticle research *22*, 1-29.

Viegas, C., Patrício, A.B., Prata, J.M., Nadhman, A., Chintamaneni, P.K., and Fonte, P. (2023). Solid Lipid Nanoparticles vs. Nanostructured Lipid Carriers: A Comparative Review. Pharmaceutics *15*, 1593.

Vieira, R., Severino, P., Nalone, L.A., Souto, S.B., Silva, A.M., Lucarini, M., Durazzo, A., Santini, A., and Souto, E.B. (2020). Sucupira oil-loaded nanostructured lipid carriers (NLC): Lipid screening, factorial design, release profile, and cytotoxicity. Molecules *25*, 685.

Xinying, W., Peng, X., Mingbiao, X., Lei, P., and Yu, Z. (2023). Synergistic improvement of foam stability with SiO2 nanoparticles (SiO2-NPs) and different surfactants. Arabian Journal of Chemistry *16*, 104394.

Yaghoobian, M., Haeri, A., Bolourchian, N., Shahhosseni, S., and Dadashzadeh, S. (2020). The impact of surfactant composition and surface charge of niosomes on the oral absorption of repaglinide as a BCS II model drug. International Journal of Nanomedicine, 8767-8781.

Yu, G., Ali, Z., Khan, A.S., Ullah, K., Jamshaid, H., Zeb, A., Imran, M., Sarwar, S., Choi, H.-G., and ud Din, F. (2023). Preparation, Pharmacokinetics, and Antitumor Potential of Miltefosine-Loaded Nanostructured Lipid Carriers [Retraction]. International Journal of Nanomedicine *18*, 1107-1108.

صياغة وتقييم ناقلات دهنية التركيب متناهية الصغر تحتوى علي عقار الريباجلينيد وذلك لتحسين الاتاحة الحيوية والخواص الفيزيائية والكيميائية للعقار

محمد أحمد نصر الدين إسماعيل إمبابي [١،٢،٣] * ابراهيم علي أبو المحاسن البهوي [١] ، أحمد محمود سامي أحمد [١]، محسن محمود السيد عفونه [١]

[١] قسم الصيدلانيات والتقنية الصيدلية، كلية الصيدلة (بنين) ، جامعة الأزهر ، ١ ش المخيم الدائم، مدينة نصر، ص.ب. صندوق بريد ١١٨٨٤، القاهرة ، مصر

[٢] الأكاديمية الطبية العسكرية

[٣] مصنع انتاج الأدوية للقوات المسلحة

* البريد الالكتروني للباحث الرئيسي: mohamednasreldin.224@azhar.edu.eg

الملخص العربى

ريباجلينيد هو دواء فعال لعلاج مرض السكري من النوع الثانى ولكنه يتمتع بتوافر حيوي عن طريق الفم أقل من ٥٥٪ بسبب ضعف قابليته للذوبان تعرضه لعملية تكسير في الكبد. الهدف من هذه الدراسة هو تطوير نظام ناقل نانوي يسمى حاملات الدهون ذات البنية النانوية المحملة بالريباجلينيد الذي يوفر فوائد إطلاق الدواء لفترة طويلة والتوافر البيولوجي المعزز عن طريق الفم. سمح إجراء تجارب الذوبان بتحديد الدهون والمواد الخافضة للتوتر السطحي المناسبة لصياغةالعينات المحضرة معمليا. تم تحضير العينات معمليا باستخدام التجانس الساخن متبوعًا بإجراءات الموجات فوق الصوتية وتم تحليلها لاحقًا من حيث الحجم والجهد السطحى للجزيئات وكذلك مؤشر تعدد التشتت وكفاءة تحميل العقار داخل الجزيئات النانوية المحضرة .أظهرت النتائج أن تغيير نوع الدهون أو المواد الخافضة للتوتر السطحي كان له تأثير كبير على كفاءات التحميل وحجم الجسيمات وسلوك إنطلاق العقار معمليا. يتراوح متوسط حجم الجسيمات بين **٥٩.١ ± ٣.٢ و ٨٩٨.٤ ± ٤٠.٣** نانومتر. تراوحت نسبة التحميل بين **٧٠.١١ ± ٥.٣** و **٨٥.٣٢ ± ٤.٦**٪. أظهرت الجسيمات شحنة سالبة، حيث تتراوح قيم شحنة السطح من ٢٣٢.٢٧. ± ١.٠١ إلى ١٢٦.١٣ ± ٧.٣٧ مللي فولت. أظهر الإنطلاق المختبري لجميع الصيغ المحضرة نمطًا ثنائي الطور يعتمد على الوقت كما أظهرت إنطلاقًا طويلًا للدواء مقارنة بالعقار نفسه دون اى إضافات. ونتيجة لذلك، تشير البيانات إلى إمكانات حاملات الدهون ذات البنية النانوية لتوصيل الأدوية عن طريق الفم، ويمكن استخدام النظام لأدوية الدرجة الثانية طبقا لنظام تصنيف المستحضرات الصيدلانية الحيوية لتحل محل الطريق الفموي التقليدي لتقليل عدد الجرعات اليومية وتحسين امتثال المريض للعلاج.

الكلمات المفتاحية : ريباجلينيد، ناقلات الدهون ذات البنية النانوية ، الاستحلاب – الموجات فوق الصوتية ، التناول عن طريق الفم.